Electronic Supplementary Material (ESI) for Analyst.

Supporting Information for: Considerations for Uranium Isotope Ratio Analysis by Atmospheric Pressure Ionization Mass Spectrometry

Thomas P. Forbes* and Christopher Szakal

National Institute of Standards and Technology, Materials Measurement Science Division, Gaithersburg, MD, USA

* Corresponding author*: E-mail:* thomas.forbes@nist.gov*; Tel: 1-301-975-2111*

Supporting Information Table of Contents

Experimental Methods

Single-element uranium dilutions. The standard ICP-MS solution was certified for mass of U, however, the uranium existed as UO_2^{2+} in solution. Dilutions of the uranium standard (10 ppm of U) were created for (4000, 1000, 400, 100, 40, 10, 4, 1) ppb of U. Given that UO_2^+ was observed as the dominant ion in the mass spectra and all isotope ratios were measured as $^{235}UO_2^+/^{238}UO_2^+$, concentration and injected mass values were converted to UO_2: (4536, 1134, 453.6, 113.4, 45.36, 11.34, 4.536, 1.134) ppb UO_2 and (22680, 5670, 2268, 567.0, 226.8, 56.70, 22.68, 5.670) pg UO_2.

Baseline subtraction. The determination of peak areas from extracted ion chronograms and subsequently isotope ratios incorporated a baseline subtraction. The instantaneous baseline background levels at the extracted ion *m/z* value were measured immediately prior to and following each discrete sample injection (*i.e.,* counts per second, cps). These before and after background levels were averaged and multiplied by the duration (*i.e.,* in seconds) of the peak of interest to give an approximation of the baseline background counts during the discrete sample injection. This background value (counts) was subtracted from the overall peak area (counts).

Supplemental Figures and Data

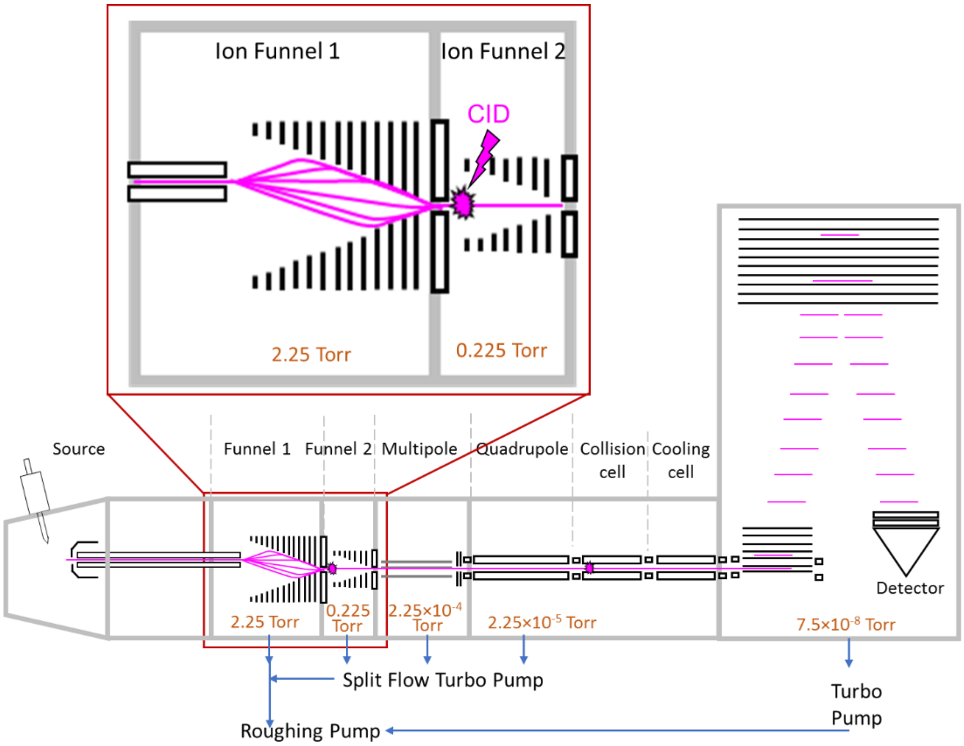

Figure S1. Schematic representation of the hybrid quadrupole time-of-flight (QTOF) mass spectrometer†. Inset represents the location of in-source collision induced dissociation (CID) between the two ion funnels. Adapted from image provided by Bruker Daltonic GmbH (Bremen, Germany).

† Certain commercial products are identified in order to adequately specify the procedure; this does not imply endorsement or recommendation by NIST, nor does it imply that such products are necessarily the best available for the purpose.

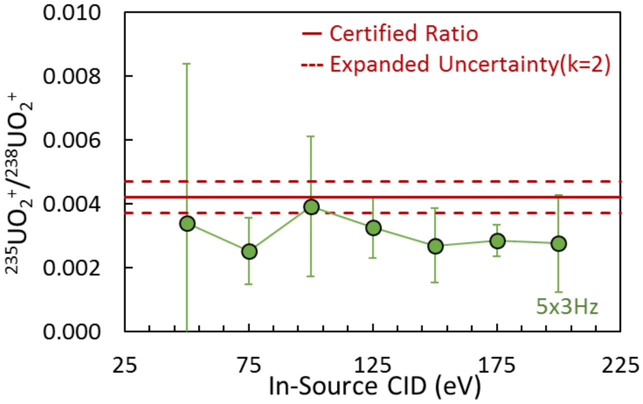

Figure S2. Isotope ratio ($^{235}UO_2^+/^{238}UO_2^+$) as a function of in-source CID energy for 567 pg UO_2 injections for spectra acquisition of 5 × 3 Hz. Data points and uncertainties represent the average peak area ratios and expanded standard deviations (k=2) of seven replicate injections at each in-source CID energy.

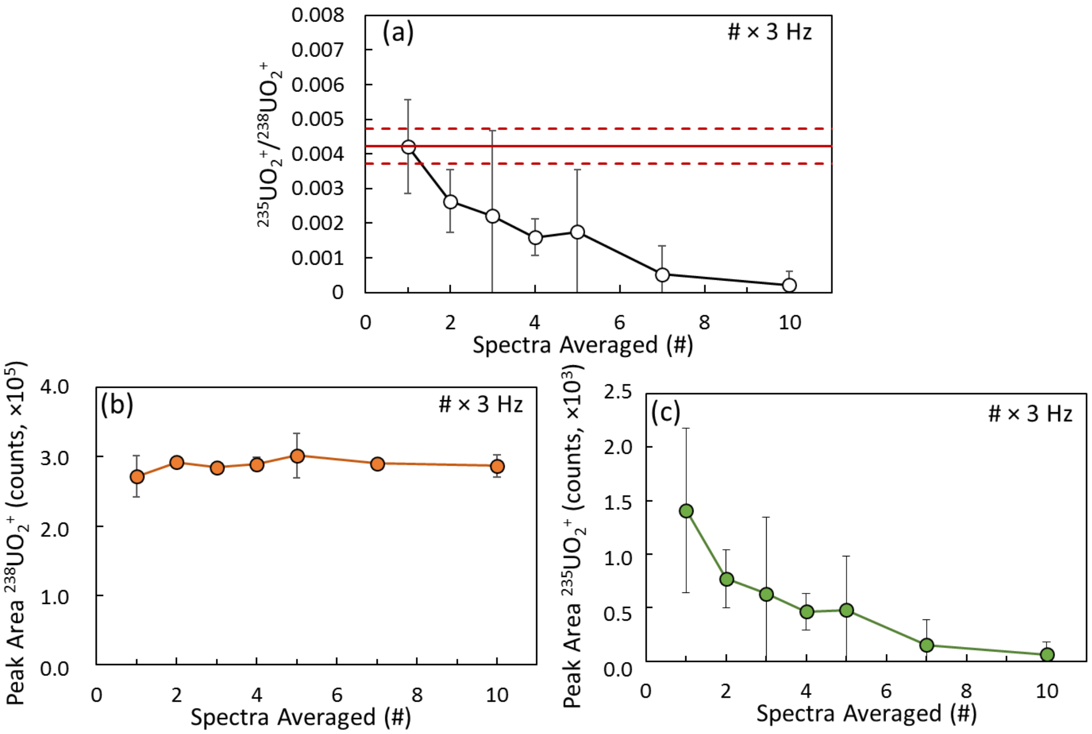

Figure S3. (a) Isotope ratio ($^{235}UO_2^+/^{238}UO_2^+$) and peak areas of (b) $^{238}UO_2^+$ and (c) $^{235}UO_2^+$ as a function of spectra averaging number for 567 pg UO_2 injections for spectra rate of 3 Hz. Data points and uncertainties expressed as averages and expanded standard deviations (k=2) of replicate injections.

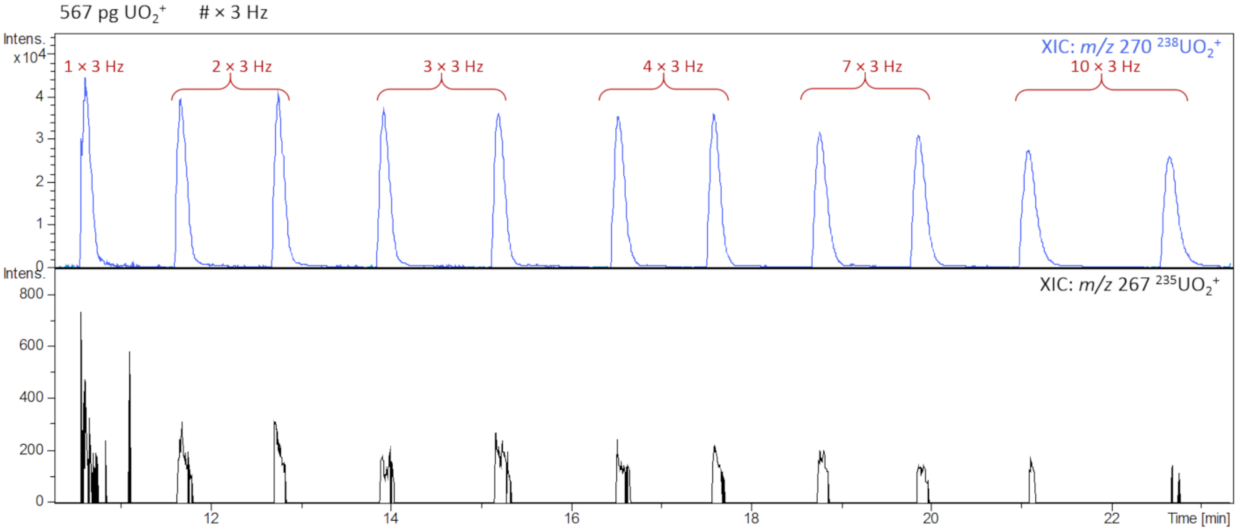

Figure S4. Examples of extracted ion chronograms (XICs) for $^{238}UO_2^+$ (*m/z* 270) and $^{235}UO_2^+$ (*m/z* 267) from 567 pg UO_2 injections as a function of spectra averaging number for a 3 Hz spectra rate.

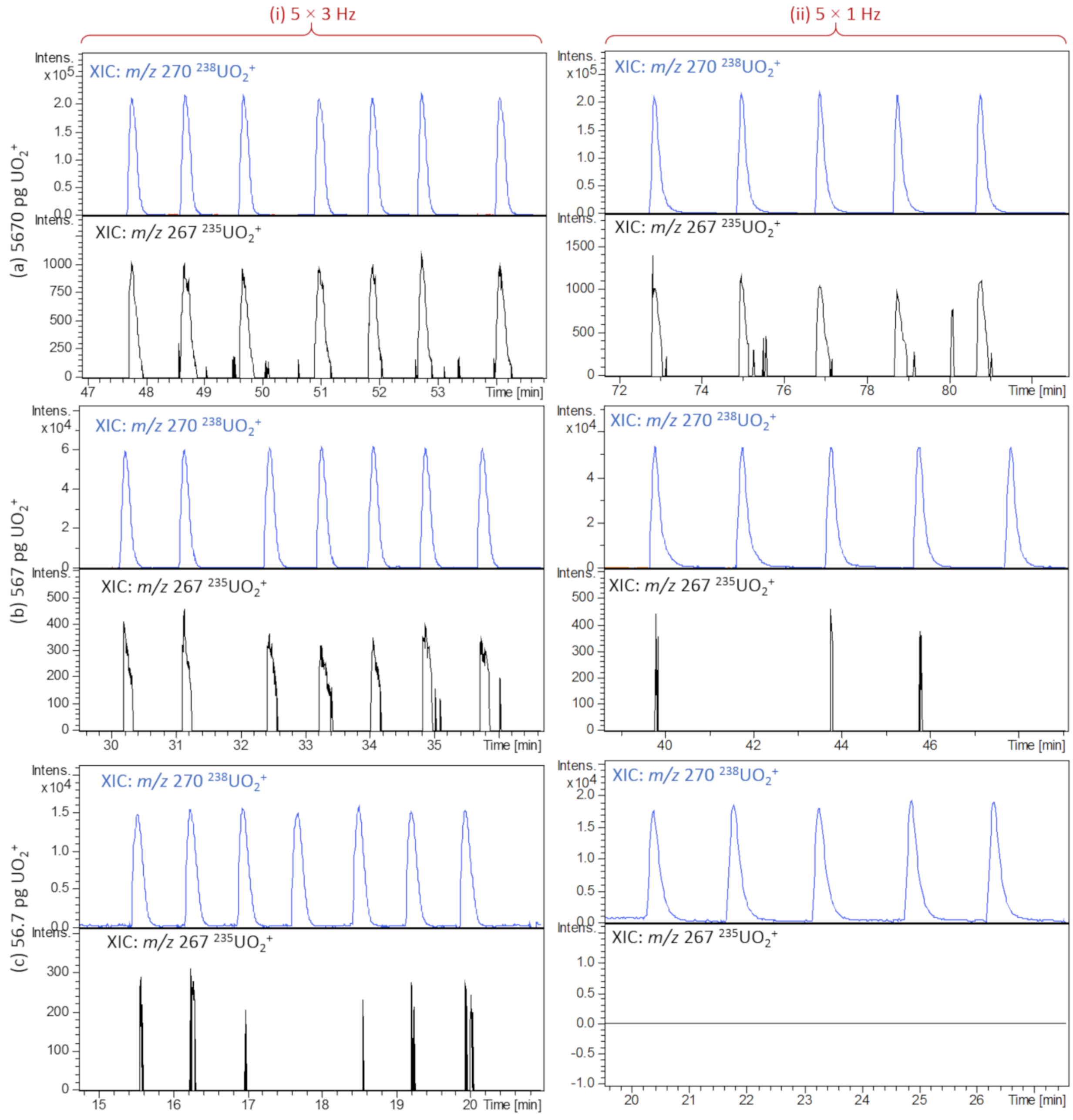

Figure S5. Examples of extracted ion chronograms (XICs) for $^{238}UO_2^+$ (*m/z* 270) and $^{235}UO_2^+$ (*m/z* 267) for UO_2 injections of (a) 5670 pg (b) 567 pg, and (c) 56.7 pg at (i) 5 × 3 Hz and (ii) 5 × 1 Hz.

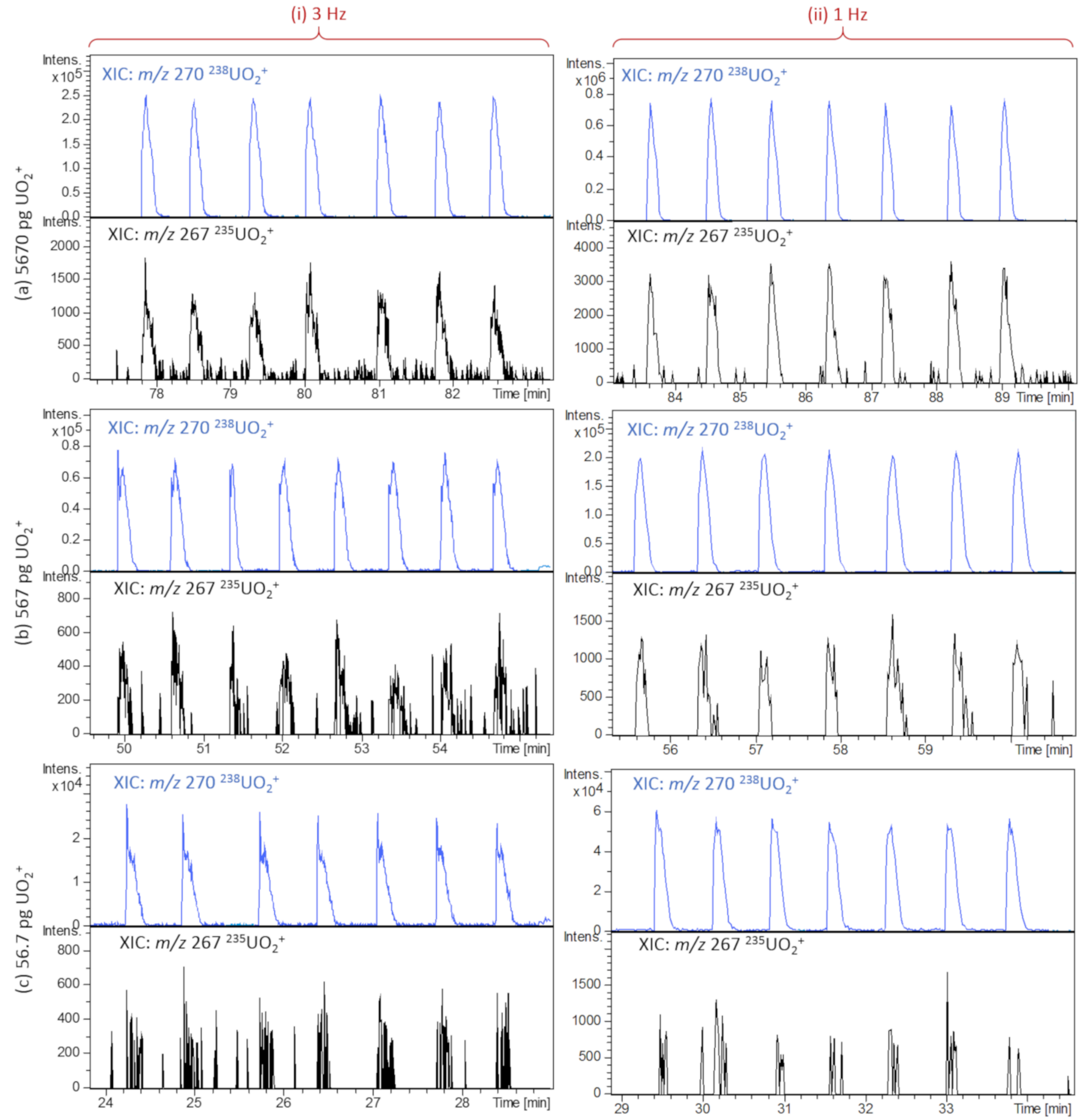

Figure S6. Examples of extracted ion chronograms (XICs) for $^{238}UO_2^+$ (*m/z* 270) and $^{235}UO_2^+$ (*m/z* 267) for UO_2 injections of (a) 5670 pg (b) 567 pg, and (c) 56.7 pg at (i) 3 Hz and (ii) 1 Hz with no averaging.

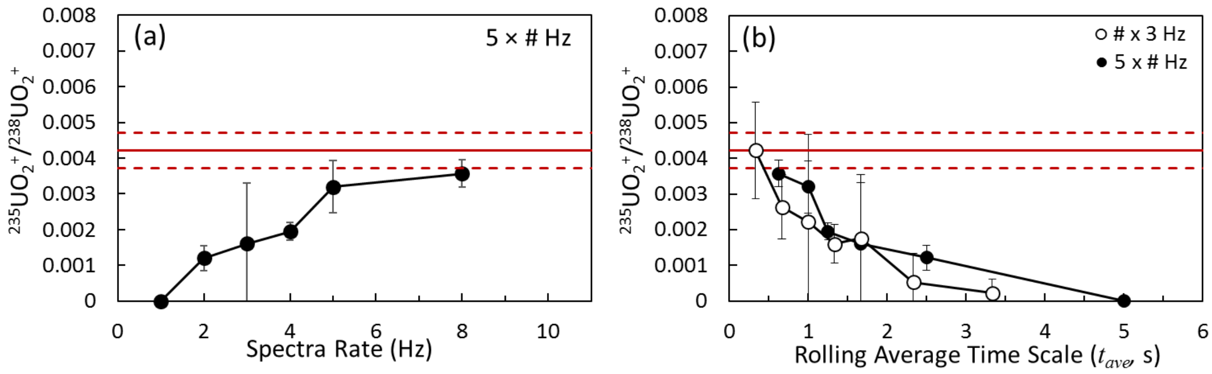

Figure S7. (a) Isotope ratio ($^{235}UO_2^+/^{238}UO_2^+$) as a function of spectra rate for 567 pg UO_2 injections and 5 spectra averaging. (b) Isotope ratio ($^{235}UO_2^+/^{238}UO_2^+$) as a function of the averaging time scale for 567 pg UO_2 injections of a series of variable spectra rates for 5 spectra averaging and variable spectra averaging for 3 Hz spectra rate. Data points and uncertainties expressed as the averages and expanded standard deviations (k=2) of replicate injections.

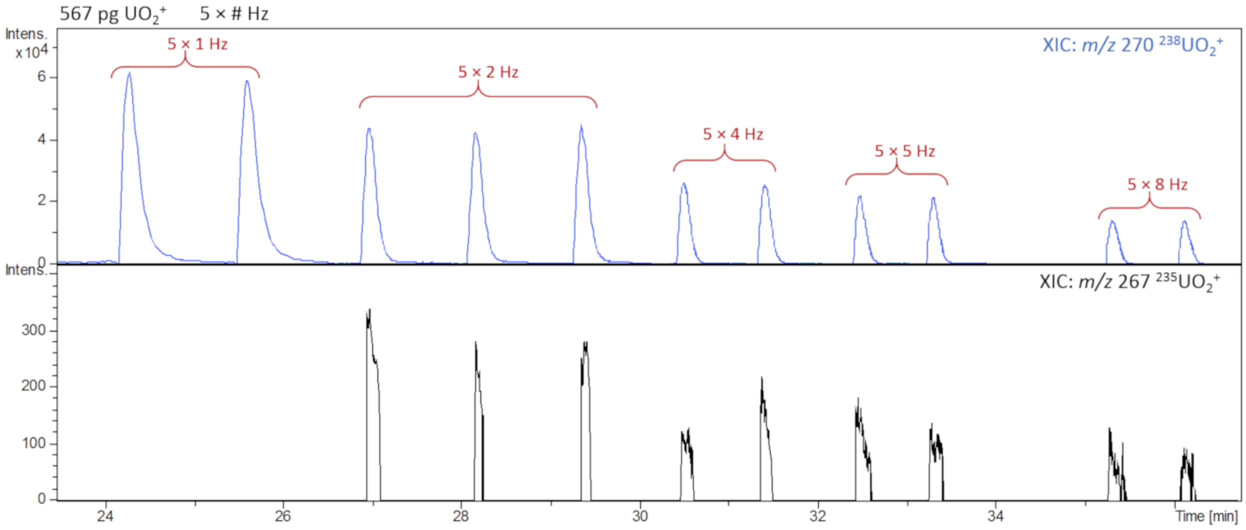

Figure S8. Examples of extracted ion chronograms (XICs) for $^{238}UO_2^+$ (*m/z* 270) and $^{235}UO_2^+$ (*m/z* 267) for 567 pg UO_2 injections as a function of spectra rate and 5 spectra averaging.

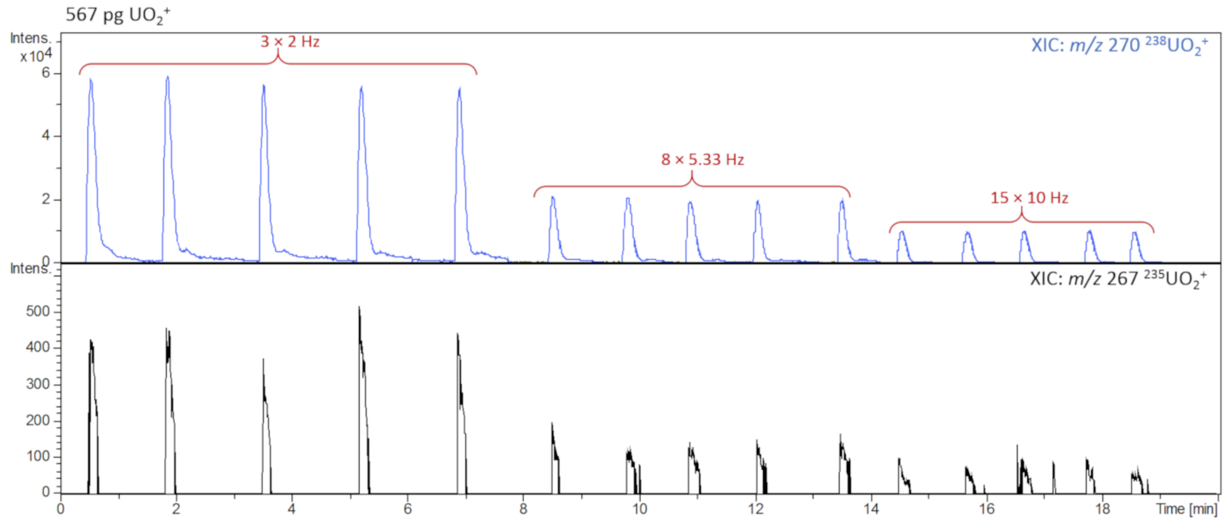

Figure S9. Examples of extracted ion chronograms (XICs) for $^{238}UO_2^+$ (*m/z* 270) and $^{235}UO_2^+$ (*m/z* 267) from 567 pg UO_2 injections for a number of spectra averaging and spectra rates, maintaining constant averaging timescale (t_{ave} = 1.5 s).

(a) Blanks prior to analysis of:

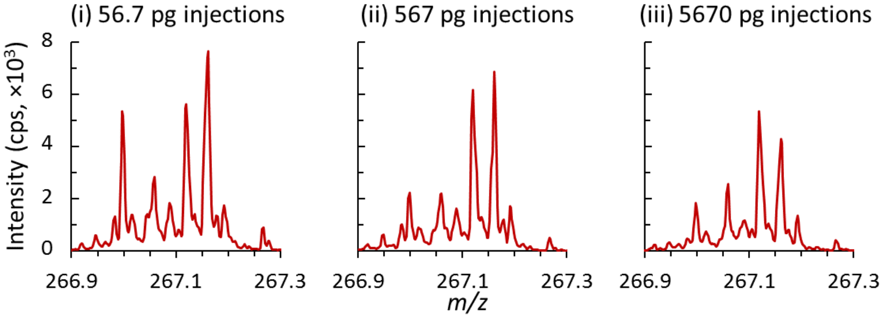

(b) UO_2 injections of:

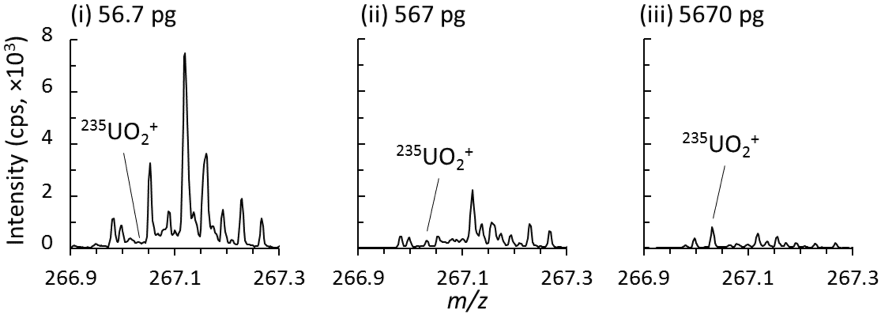

Figure S10. Examples of mass spectra in the region around $^{235}UO_2^+$ (*m/z* 267) from (a) blank injections prior to the analysis of (i) 56.7 pg, (ii) 567 pg, and (iii) 5670 pg injection replicates and (b) UO_2 injections of (i) 56.7 pg, (ii) 567 pg, and (iii) 5670 pg (Figure S10(b) matches mass spectra insets from Figure 5 with the intensity scale adjusted for visualization and comparison with S10(a)).

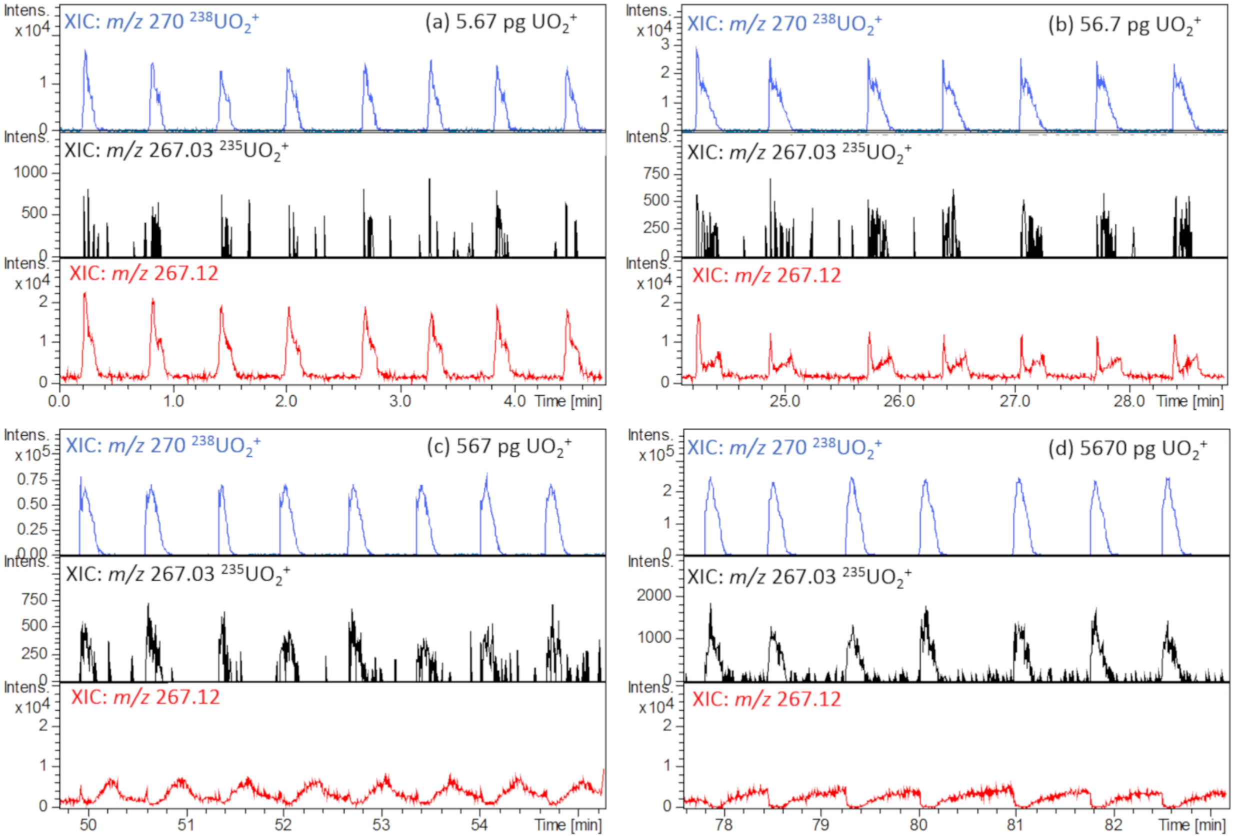

Figure S11. Examples of extracted ion chronograms (XICs) for $^{238}UO_2^+$ (*m/z* 270.04) and $^{235}UO_2^+$ (*m/z* 267.03) and a chemical noise peak (*m/*z 267.12) for UO_2 injections of (a) 5.67 pg (b) 56.7 pg, and (c) 567 pg and (d) 5670 pg at 3 Hz with no averaging.

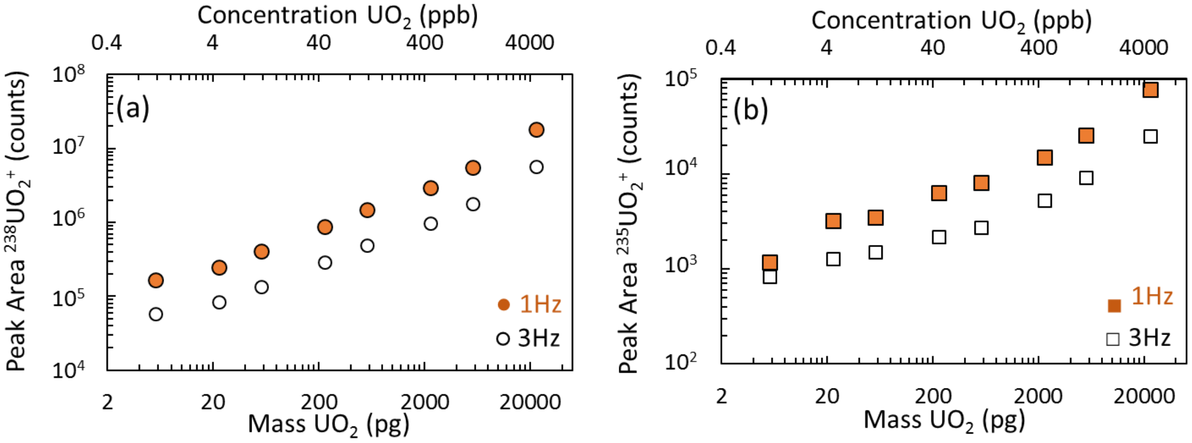

Figure S12. Peak areas of (a) $^{238}UO_2^+$ and (b) $^{235}UO_2^+$ as a function of UO_2 injection mass 1 Hz and 3 Hz spectra rates. Data points and uncertainties expressed as the averages and expanded standard deviations (k=2) of seven replicate injections. Uncertainties are smaller than data points.